Journal of Alloys and Compounds 505 (2010) 423–427

Contents lists available at ScienceDirect

Journal of Alloys and Compounds

journal homepage: www.elsevier.com/locate/jallcom

Structural and magnetic investigation of $(R_{1-x}R'_x)_2Fe_{17-y}Co_yN_z$ powders by Mössbauer spectrometry

F. Richomme [a], J.M. Le Breton [a,*], M.S. Ben Kraiem [b], M. Ellouze [c], A. Cheikhrouhou [d], Ph. L'Héritier [e]

[a] Groupe de Physique des Matériaux, UMR 6634 CNRS, Université de Rouen, 76801 Saint-Etienne du Rouvray, France
[b] SETIT, Institut Préparatoire aux Etudes d'Ingénieurs de Sfax, 3018 Sfax, Tunisia
[c] SETIT, Faculté des Sciences de Sfax, Université de Sfax, 3038 Sfax, Tunisia
[d] Faculté des Sciences de Sfax, B.P. 1171, 3000 Sfax, Tunisia
[e] Laboratoire des Matériaux et du Génie Physique, PHELMA, Grenoble INP, Minatec, 38016 Grenoble, France

ARTICLE INFO

Article history:
Received 8 April 2010
Received in revised form 9 June 2010
Accepted 12 June 2010
Available online 25 June 2010

Keywords:
Rare-earth transition metal compounds
Nitrogenation
Mössbauer

ABSTRACT

$(R_{1-x}R'_x)Fe_{17-y}Co_y$ powders were prepared by induction melting. Nitrogen (2.9 ± 0.1 atoms per formula unit) was inserted under a static nitrogen gas atmosphere. The nitrided powders have been investigated by ^{57}Fe Mössbauer spectrometry and X-ray diffraction. The analyses show that the samples are composed of two phases: the nitrided $(R_{1-x}R'_x)Fe_{17-y}Co_yN_z$ phase and α-Fe. The variations of the Mössbauer hyperfine parameters of the nitrided phase are explained both by the lattice expansion and by the presence of nitrogen. The observed variations do not indicate an influence of the rare-earth on the isomer shift. Nitrogenation increases the hyperfine field at the Fe sites in agreement with the enhancement of the Curie temperature.

1. Introduction

Experimental investigations of nitrided R_2Fe_{17} and $R_2(Fe_{1-x}Co_x)_{17}$ compounds have shown that their magnetic properties can be remarkably improved by the introduction of interstitial nitrogen atoms [1–4]. Nitrogenation induces a volume expansion of the lattice between 3% and 7%, leading to a large enhancement of both Curie temperature and magnetization [5,6]. Like their unnitrided counterparts, the $R_2Fe_{17}N_z$ compounds crystallize in a rhombohedral Th_2Zn_{17} structure for light rare-earths (Pr, Nd, Sm) [5,6], the nitrogen atoms being located predominantly on the 9e site [7].

Nitrogenation can also induce a change of the magnetocrystalline anisotropy. The magnetocrystalline anisotropy of R_2Fe_{17} compounds depends on the nature of the rare-earth, that is, on the symmetry of the 4f charge distribution (a rare-earth atom carries a localised magnetic moment due to 4f electrons). The α_J second order Stevens coefficient characterizes the asphericity of the 4f shell [8]. When $\alpha_J > 0$ (as for Sm: $\alpha_J \langle r_{4f}^2 \rangle = +40.209 \times 10^{-3} a_0^2$), the shape of the electronic distribution is prolate, i.e. elongated along the moment direction. When $\alpha_J < 0$ (as for Nd: $\alpha_J \langle r_{4f}^2 \rangle = -7.161 \times 10^{-3} a_0^2$), the 4f electron charge distribution is oblate, i.e. expanded perpendicular to the moment direction. For $\alpha_J = 0$, which is the case of the Gd^{3+} ion, the charge density has spherical symmetry. In R_2Fe_{17} compounds, the Fe sub-lattice anisotropy is strong. Thus, even if the Sm moment seems to prefer the *c*-axis, the Sm_2Fe_{17} compound shows planar anisotropy [3]. Consequently, the magnetocrystalline anisotropy of Nd_2Fe_{17}, Sm_2Fe_{17} and Gd_2Fe_{17} compounds is planar at room temperature. However, while the anisotropy of $Nd_2Fe_{17}N_z$ and $Gd_2Fe_{17}N_z$ compounds remain planar at room temperature, $Sm_2Fe_{17}N_z$ presents an uniaxial magnetic anisotropy [9,10].

With the aim of investigating the influence of nitrogenation on the iron sub-lattice, we investigated $Nd_{2-x}Sm_xFe_{17}N_z$ ($x = 0$, 1, 1.5, 2), $NdGdFe_{17}N_z$, $Nd_2Fe_{16}CoN_z$ and $Nd_{1.5}Gd_{0.5}Fe_{16}CoN_z$ powders using Mössbauer spectrometry. The Mössbauer spectra of the corresponding unnitrided powders have been reported before [11]. The structure of the samples has been investigated by X-ray diffraction. Magnetic measurements have been previously done on the same samples to determine Curie temperature and saturation magnetization [5,6,12].

2. Experimental

$(R_{1-x}R'_x)_2Fe_{17-y}Co_y$ compounds were prepared from starting materials of at least 99.9% purity by induction melting. After melting, the polycrystalline specimens were sealed in silica tubes under argon atmosphere, annealed at 1273 K for 10 days and then quenched in water. The insertion of nitrogen has been carried out in static nitrogen gas under a pressure of 15 MPa at 733 K for 24 h. The nitrogen content was checked by the weight increase in the samples. It was found to be 2.9 ± 0.1 atoms per formula unit [5,6,12].

* Corresponding author. Tel.: +33 2 32 95 50 39; fax: +33 2 32 95 50 32.
E-mail address: jean-marie.lebreton@univ-rouen.fr (J.M. Le Breton).

0925-8388/$ – see front matter © 2010 Elsevier B.V. All rights reserved.
doi:10.1016/j.jallcom.2010.06.108

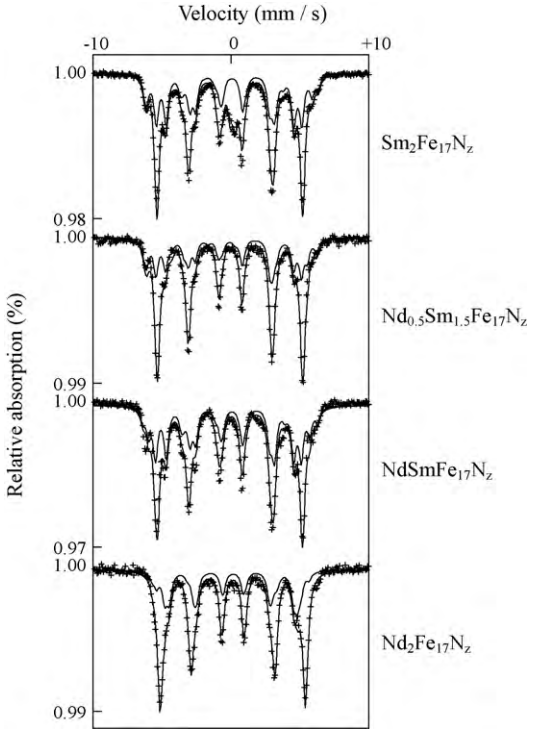

Fig. 1. Room temperature Mössbauer spectra of the $Sm_2Fe_{17}N_z$, $Nd_{0.5}Sm_{1.5}Fe_{17}N_z$, $NdSmFe_{17}N_z$ and $Nd_2Fe_{17}N_z$ samples. The contribution of the $R_2Fe_{17}N_z$ phase is displayed in each spectrum.

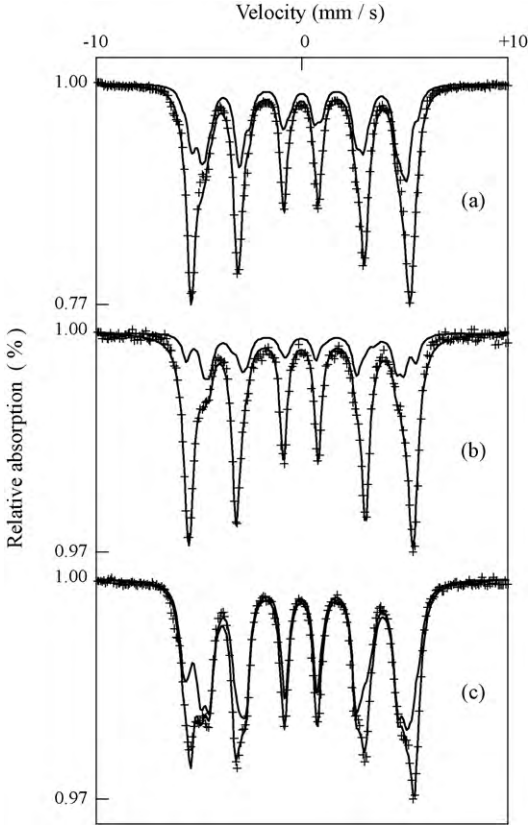

Fig. 2. Room temperature Mössbauer spectra of the $NdGdFe_{17}N_z$ (a), $Nd_{1.5}Gd_{0.5}Fe_{16}CoN_z$ (b) and $Nd_2Fe_{16}CoN_z$ (c) samples. The contribution of the $R_2Fe_{17}N_z$ phase is displayed in each spectrum.

X-ray diffraction (XRD) analysis was performed in the angular range $2\theta = 20–90^\circ$. For these experiments a Brucker D8 powder diffractometer with the Co($K\alpha_1$) radiation ($\lambda = 0.1788970$ nm) was used.

All the samples were investigated by Mössbauer spectrometry at room temperature, using a conventional spectrometer with a ^{57}Co source in a rhodium matrix. The isomer shifts δ are relative to metallic iron at room temperature. The hyperfine field is denoted B. The errors were obtained from the fitting program [13], being estimated to ±0.05 mm/s for the isomer shift and ±0.5 T for the hyperfine field.

3. Results

The room temperature Mössbauer spectra of the samples are reported in Figs. 1 and 2. These spectra reveal the presence of two contributions: the contribution of the nitrided compound and the contribution of α-Fe. The contribution of the nitrided phase is displayed in both figures. The presence of α-Fe is confirmed by XRD analysis. For example, the XRD pattern of the $Nd_2Fe_{16}CoN_z$ sample is presented in Fig. 3. In the pattern, in addition to the peaks of the nitrided compound, the main peak of the α-Fe and a peak corresponding to Nd-rich phases are clearly observed. These results show that the nitrogenation process leads to a partial decomposition of the 2:17 phase into α-Fe and Nd-rich phases. The Mössbauer relative intensities of these contributions, reported in Table 1, indicate that the α-Fe contribution can be important. However, because the hyperfine parameters of the contribution of α-Fe are well determined, this contribution can be distinguished from that of the nitrided phase, allowing an accurate fit of the contribution of the nitrided phase.

Table 1
Mössbauer relative intensity of the contributions used to fit the room temperature spectra of the samples.

Sample	Nitrided R_2Fe_{17} phase	α-Fe (Co)	Paramagnetic phase
$Sm_2Fe_{17}N_z$	53	40	7
$Nd_{0.5}Sm_{1.5}Fe_{17}N_z$	46	54	–
$NdSmFe_{17}N_z$	59	41	–
$Nd_2Fe_{17}N_z$	52	48	–
$NdGdFe_{17}N_z$	48	52	–
$Nd_{1.5}Gd_{0.5}Fe_{16}CoN_z$	27	73	–
$Nd_2Fe_{16}CoN_z$	81	19	–

3.1. Fitting procedure

The Mössbauer contribution of the nitrided phase has been fitted according to both the crystal structure and the magnetocrystalline anisotropy of the compounds, in agreement with what has been done for unnitrided $(R_{1-x}R'_x)Fe_{17-y}Co_y$ compounds [11].

The Mössbauer spectra of the $Sm_2Fe_{17}N_z$ and $Sm_{1.5}Nd_{0.5}Fe_{17}N_z$ phases were fitted with four sextets corresponding to the 18f, 18h, 9d, and 6c Fe sites, in agreement with the fact that the magnetic

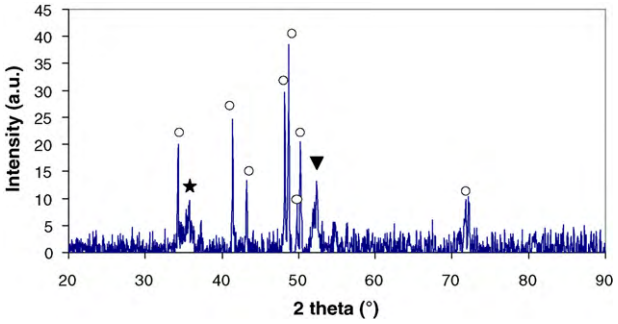

Fig. 3. XRD pattern of the $Nd_2Fe_{16}CoN_x$ sample. The peaks indexed by (○) are the main peaks of the $Nd_2Fe_{16}CoN_3$ phase. The peak indexed by (▼) is the main peak of the α-Fe phase. The peak indexed by (★) corresponds to the Nd-rich phase.

Table 2
Room temperature isomer shifts (in mm/s) obtained for the contribution of the nitrided phase, for the different samples.

Sample	18f	18h	9d	6c	Mean value
$Sm_2Fe_{17}N_z$	0.03	0.08	−0.09	0.17	0.043
$Sm_2Fe_{17}N_z$ (after [14])	0.04	0.12	−0.07	0.16	0.063
$Sm_2Fe_{17}N_z$ (after [15])	0.05	−0.01	−0.09	0.12	0.012
$Nd_{0.5}Sm_{1.5}Fe_{17}N_z$	0.02	0.06	−0.10	0.12	0.014
$NdSmFe_{17}N_z$	0.09	0.08	−0.11	0.16	0.060
$Nd_2Fe_{17}N_z$	0.08	0.05	−0.11	0.11	0.077
$Nd_2Fe_{17}N_z$ (after [3])	0.075	0.100	−0.100	0.175	0.064
$NdGdFe_{17}N_z$	0.08	0.10	−0.15	0.19	0.058
$Nd_{1.5}Gd_{0.5}Fe_{16}CoN_z$	0.06	0.09	−0.06	0.14	0.059
$Nd_2Fe_{16}CoN_z$	0.09	0.09	−0.06	0.20	0.074

anisotropy of the corresponding Sm-rich nitrided compounds is uniaxial [9,10]. In addition, as for the unnitrided Sm_2Fe_{17} sample [11], a central paramagnetic component was introduced for the spectrum of the $Sm_2Fe_{17}N_z$ sample to account for the extra absorption at the centre of the spectrum. This contribution could correspond to an R–Fe–O oxide or to a nanocrystalline R–Fe phase

The Mössbauer spectrum of the $NdGdFe_{17}N_z$ phase was fitted with seven sextets, namely: $18f_{12}$, $18f_6$, $18h_{12}$, $18h_6$, $9d_6$, $9d_3$ and 6c, as for the unnitrided materials [11]. Indeed, the magnetization remains in the basal plane along the [1 0 0] axis in $Nd_2Fe_{17}N_x$ [9]. We assume that this result is also valuable for $NdGdFe_{17}N_z$.

The Mössbauer spectra of the $Nd_{1.5}Gd_{0.5}Fe_{16}CoN_z$ and $Nd_2Fe_{16}CoN_z$ phases were fitted with four sextets corresponding to the 18f, 18h, 9d, and 6c Fe sites, as for the unnitrided $R_2Fe_{16}Co$ samples, with the same proportions for the different Fe sites [11].

3.2. Isomer shift

The isomer shifts of the different Fe sites in the nitrided phase are listed in Table 2. The values obtained for $Sm_2Fe_{17}N_z$ and $Nd_2Fe_{17}N_z$ can be compared with the values obtained from the literature [3,14,15]. A very good agreement is observed.

For all the samples we note that $\delta(6c) > \delta(18h) > \delta(18f) > \delta(9d)$. This order has also been observed in other $R_2Fe_{17}N_x$ compounds [3,14–16]. In general, the larger the Wigner–Seitz cell volume of a site, the larger the isomer shift. So the order would be $\delta(6c) > \delta(18h) > \delta(9d) > \delta(18f)$ [14]. Structural considerations indicate that the interstitial sites large enough to accommodate nitrogen atoms (the pseudooctahedral 9e sites) have only 18f and 18h near neighbours [3]. Nitrogenation leads to an expansion of the lattice. On the other hand, nitrogen, which is more electronegative than iron, tends to increase the isomer shift of neighbouring sites. In agreement with these considerations, the δ values increase upon nitrogenation for all the Fe sites.

To discuss the results, we report in Table 4 the variation of the isomer shift $\Delta\delta = \delta_{\text{nitrided sample}} - \delta_{\text{unnitrided sample}}$ for each Fe site. The most important variation is obtained for the 18h site, followed by the 18f site. The variations obtained for the 9d and 6c sites are much lower than the others. We assume that the increase of δ(9d) and δ(6c) is only due to the lattice expansion. The increase of δ(18f) is attributed to the presence of nitrogen near neighbours only, because the Wigner–Seitz cell does not vary upon nitrogenation for this site. The increase of δ(18h) is attributed to both phenomena. This is in agreement with other studies [3,17]. It is worth to mention that the values obtained for the different sites and for the different samples do not indicate an influence of the rare-earth, as for the unnitrided samples [11].

3.3. Hyperfine field

The hyperfine fields of the different Fe sites in the nitrided phase are listed in Table 3. The values obtained for $Sm_2Fe_{17}N_z$ and $Nd_2Fe_{17}N_z$ can be compared with the values obtained from the literature [1,3,14,15]. A very good agreement is observed.

Compared to the unnitrided samples [11], the hyperfine field increases for each Fe site in the nitrided compounds. The increase of the hyperfine field is related to the increase of the Curie temperature. It has been demonstrated that nitrogenation increases the Curie temperature of these materials by about 400° [18]. This is related to the expansion of the lattice upon nitrogenation, which enhances the Fe–Fe ferromagnetic coupling. Thus, T_c increases with the average Fe–Fe distance [19]. For example, T_c increases from 400 K for Sm_2Fe_{17} up to 780 K for $Sm_2Fe_{17}N_3$ [20], and the average hyperfine field increases from 21.55 T for Sm_2Fe_{17} to 33.15 T for $Sm_2Fe_{17}N_3$ (Table 3). For $NdGdFe_{17}$, nitrogenation increases T_c from 400 K up to 768 K for $NdGdFe_{17}N_{2.8}$ [6], and the room temperature magnetization increases from 24.10 μ_B/fu to 35.08 μ_B/fu [6].

For the unnitrided compounds there is a correlation between the value of the hyperfine field and the number of iron near neighbours for each site. The same correlation is obtained for the nitrided compounds. Indeed, we observe that $B(6c) > B(9d) > B(18f) > B(18h)$ for all the samples as in $Sm_2Fe_{17}N_x$ [1,14,15]. The observed sequence of hyperfine field is also in agreement with the sequence

Table 3
Room temperature hyperfine fields (in T) obtained for the contribution of the nitrided phase, for the different samples.

Sample	18f	18h	9d	6c	Mean value
$Sm_2Fe_{17}N_z$	33.0	29.1	37.5	39.3	33.2
$Sm_2Fe_{17}N_z$ (after [1])	33.3	29.5	37.3	39.0	33.3
$Sm_2Fe_{17}N_z$ (after [14])	33.7	29.7	37.8	39.4	33.7
$Sm_2Fe_{17}N_z$ (after [15])	33.0	29.0	36.8	38.9	32.9
$Nd_{0.5}Sm_{1.5}Fe_{17}N_z$	33.1	29.2	36.5	39.1	33.0
$NdSmFe_{17}N_z$	33.2	29.1	36.7	38.9	33.0
$Nd_2Fe_{17}N_z$	30.2	28.3	32.9	35.8	30.7
$Nd_2Fe_{17}N_z$ (after [1])	31.2	28.7	34.1	36.9	31.5
$Nd_2Fe_{17}N_z$ (after [3])	29.0	31.4	35.8	34.3	31.7
$NdGdFe_{17}N_z$	31.2	29.4	32.8	34.8	31.3
$Nd_{1.5}Gd_{0.5}Fe_{16}CoN_z$	30.4	28.4	34.8	35.0	31.0
$Nd_2Fe_{16}CoN_z$	31.3	28.6	34.8	35.1	31.4

Table 4
Variation of the isomer shift $\Delta\delta$ (in mm/s) for each Fe site for the samples investigated. The values obtained for the unnitrided samples are taken from [11].

Sample	18f	18h	9d	6c
$Sm_2Fe_{17}N_z$	+0.13	+0.17	+0.10	+0.08
$NdSmFe_{17}N_z$	+0.18	+0.16	+0.07	+0.06
$Nd_2Fe_{17}N_z$	+0.15	+0.10	+0.06	+0.00
$Nd_{1.5}Gd_{0.5}Fe_{16}CoN_z$	+0.16	+0.17	+0.10	+0.00
$Nd_2Fe_{16}CoN_z$	+0.18	+0.18	+0.06	+0.12

of magnetic moments calculated for $Gd_2Fe_{17}N_3$ [21] and for $Y_2Fe_{17}N_3$ [22]. In $Nd_2Fe_{17}N_{2.6}$ [3], it has been reported that $B(9d) > B(6c) > B(18h) > B(18f)$.

To discuss these results, we report the relative variation of the hyperfine field $\Delta B/B = (B_{\text{nitrided sample}} - B_{\text{unnitrided sample}})/B_{\text{unnitrided sample}}$ in Table 5. For all the samples, the largest increase of $\Delta B/B$ is observed for the 9d Fe site. This result is in agreement with calculated electronic and magnetic structures of $Nd_2Fe_{17}N_3$ [23] and $Y_2Fe_{17}N_3$ [22] compounds where it has been found that the magnetic moment of the 9d Fe atoms is the most enhanced upon nitrogenation. Indeed all the distances between the 9d site and their iron near neighbours increase upon nitrogenation, thus improving the ferromagnetic exchange between theses sites and their near neighbours. For example, neutron diffraction experiments performed in $Y_2Fe_{17}N_z$ compounds revealed at 10 K a strong enhancement of the magnetic moments of the Fe atoms in the 6c sites ($\mu_{Fe}(6c) = 2.23\,\mu_B$ for Y_2Fe_{17} and $2.86\,\mu_B$ for $Y_2Fe_{17}N_3$ [24,25]), in relation with the fact that Fe atoms in the 6c site are the farthest ones from the 9e-N atoms. Calculations of the electronic and magnetic structures of Nd_2Fe_{17} and $Nd_2Fe_{17}N_3$ show that upon nitrogenation, the moments of the nearest neighbours Fe(18f) and Fe(18h) are reduced and the moment of the next-nearest neighbour Fe(9d) increases [23].

From the values reported in Table 5, one can notice that for each Fe site, the value of $\Delta B/B$ increases with the Nd content. This is in agreement with the variation of T_c with the composition: the relative increase of T_c is lower for Sm_2Fe_{17} than for Nd_2Fe_{17} (400–780 K upon nitrogenation of Sm_2Fe_{17} [20], compared with 330–743 K upon nitrogenation of Nd_2Fe_{17} [6]). The same observation can be made for the Co-containing samples: the relative increase of T_c is lower for $Nd_{1.5}Gd_{0.5}Fe_{16}Co$ than for $Nd_2Fe_{16}Co$ (504–795 K upon nitrogenation of $Nd_{1.5}Gd_{0.5}Fe_{16}Co$ [12], compared with 441–773 K upon nitrogenation of $Nd_2Fe_{16}Co$ [12]). Thus, as for the unnitrided samples [11], the variation of the hyperfine field has to be related to the variation of T_c with the composition.

It is worth mentioning that the relative increase of the hyperfine field is lower for the Co-containing samples than for the Co-free samples (see Table 5). This is attributed to the fact that the T_c of the Co-containing samples is higher than the T_c of the corresponding Co-free samples, thus inducing a lower relative increase of their hyperfine field upon nitrogenation than for the Co-free counterparts. For example, the T_c of the $Nd_2Fe_{16}Co$ sample increases from 441 K to 773 K upon nitrogenation [12], while that of the Nd_2Fe_{17} sample increases from 330 K to 743 K [6].

Table 5
Relative variation of the hyperfine field $\Delta B/B$ (in %) for each Fe site for the samples investigated. The values obtained for the unnitrided samples are taken from [11].

Sample	18f	18h	9d	6c
$Sm_2Fe_{17}N_z$	53	46	71	51
$NdSmFe_{17}N_z$	73	59	85	68
$Nd_2Fe_{17}N_z$	90	78	102	79
$Nd_{1.5}Gd_{0.5}Fe_{16}CoN_z$	13	16	26	12
$Nd_2Fe_{16}CoN_z$	31	25	35	25

Table 6
Room temperature quadrupolar shift ε (in mm/s) for the 6c site, obtained from the Mössbauer contribution of the nitrided phase in the $Nd_{2-x}Sm_xFe_{17}N_z$ samples.

x	ε
0	−0.07
1	−0.15
1.5	0.34
2	0.15

3.4. Magnetic anisotropy of $Nd_{2-x}Sm_xFe_{17}N_z$ compounds

Previous investigations revealed that the magnetocrystalline anisotropy of $Nd_2Fe_{17}N_z$ is planar at room temperature, while that of $Sm_2Fe_{17}N_z$ is uniaxial. The magnetic anisotropy of $Nd_{2-x}Sm_xFe_{17}N_z$ compounds can be investigated from the quadrupolar shift ε of the contribution of Fe atoms in the 6c site. The quadrupolar shift can be expressed as: $\varepsilon = eQVzz/4\,(3\cos^2\theta - 1 + \eta\sin^2\theta\cos(2\phi))$, where θ is the angle between the magnetic moments and the c-axis and ϕ the angle between the projection of the magnetic moments and the a-axis in the basal plane. The values reported in Table 6 indicate that the magnetic moments of iron are in the basal plane for $Nd_2Fe_{17}N_z$ and $NdSmFe_{17}N_z$ ($\varepsilon < 0$ and $\theta = 90°$), and along the c-axis for the $Nd_{0.5}Sm_{1.5}Fe_{17}N_z$ and $Sm_2Fe_{17}N_z$ ($\varepsilon > 0$ and $\theta = 0°$). This indicates that the change in magnetocrystalline anisotropy of the $Nd_{2-x}Sm_xFe_{17}N_z$ compounds occurs between $x = 1$ and $x = 1.5$.

4. Conclusion

$Nd_{2-x}Sm_xFe_{17}N_z$ ($x = 0$, 1, 1.5, 2), $NdGdFe_{17}N_z$, $Nd_2Fe_{16}CoN_z$ and $Nd_{1.5}Gd_{0.5}Fe_{16}CoN_z$ powders were investigated by Mössbauer spectrometry. The analyses show that the samples are composed of two phases: the nitrided $(R_{1-x}R'_x)Fe_{17-y}Co_yN_z$ phase and α-Fe. The variations of the isomer shifts upon nitrogenation are explained both by the lattice expansion and by the presence of nitrogen: the increase observed for the 9d and 6c Fe sites is due to the expansion of the lattice, the increase observed for the 18f site is only due to the presence of nitrogen as near neighbour, and the increase observed for the 18h site is attributed to both effects. These variations do not indicate an influence of the rare-earth on the isomer shift, in agreement with the enhancement of the Curie temperature. Compared to the unnitrided phases, nitrogenation induces an increase of the hyperfine field at the Fe sites that follows the increase of the Curie temperature. The largest increase is observed for the 9d Fe site, in agreement with the literature. In $Nd_{2-x}Sm_xFe_{17}N_z$ compounds, a change in magnetocrystalline anisotropy from the basal plane towards the c-axis is observed between $x = 1$ and $x = 1.5$.

References

[1] B.-P. Hu, H.-S. Li, H. Sun, J.M.D. Coey, Journal of Physics: Condensed Matter 3 (1991) 3983.
[2] V.K. Agarval, R.N. Kuz'min, Soviet Physics Crystallography 16 (1972) 670.
[3] G.J. Long, O.A. Pringle, F. Grandjean, K.H.J. Buschow, Journal of Applied Physics 72 (1992) 4845.
[4] J.F. Herbst, J.J. Croat, R.W. Lee, W.B. Yelon, Journal of Applied Physics 53 (1982) 250.
[5] M.S. Ben Kraiem, A. Cheikhrouhou, Physica Status Solidi (c) 3 (2006) 3233.
[6] M.S. Ben Kraiem, M. Ellouze, A. Cheikh-Rouhou, Ph. L'Héritier, Journal of Alloys and Compounds 363 (2004) 19.
[7] T. Kajitani, Y. Morii, S. Funahashi, H. Kato, Y. Nakagawa, K. Hiraya, Journal of Applied Physics 73 (1993) 6032.
[8] J.J.M. Franse, R.J. Radwanski, in: K.H.J. Buschow (Ed.), Handbook of Magnetic Materials, vol. 7, 1993, p. 307.
[9] H. Sun, J.M.D. Coey, Y. Otani, D.P.F. Hurley, Journal of Physics: Condensed Matter 2 (1990) 6465.
[10] T. Iriyama, K. Kobayashi, N. Imaoka, T. Fukuda, H. Kato, Y. Nakagawa, IEEE Transactions on Magnetics 28 (1992) 2326.
[11] F. Richomme, J.M. Le Breton, M.S. Ben Kraiem, A. Cheikhrouhou, Journal of Alloys and Compounds 494 (2010) 5–10.

[12] M.S. Ben Kraiem, M. Ellouze, A. Cheikh-Rouhou, Ph. L'Héritier, Physica Status Solidi (c) 7 (2004) 1706.
[13] J. Teillet, F. Varret, Unpublished MOSFIT Program, 1983.
[14] G.J. Long, S. Misshra, O.A. Pringle, F. Grandjean, K.H.J. Buschow, Journal of Applied Physics 75 (1994) 5994.
[15] R.J. Zhou, M. Rosenberg, M. Katter, L. Schultz, Journal of Magnetism and Magnetic Materials 118 (1993) 110.
[16] O.A. Pringle, G.J. Long, F. Grandjean, K.H.J. Buschow, Journal of Magnetism and Magnetic Materials 104–107 (1992) 1123.
[17] V. De Pauw, D. Lemarchand, A. Fnidiki, Journal of Magnetism and Magnetic Materials 169 (1997) 82.
[18] J.M.D. Coey, H. Sun, Journal of Magnetism and Magnetic Materials 87 (1990) L251.
[19] O. Isnard, S. Miraglia, D. Fruchart, J. Deportes, P. L'Heritier, Journal of Magnetism and Magnetic Materials 131 (1994) 76.
[20] K.H.J. Buschow, R. Coehoorn, D.B. de Moij, K. de Waard, T.H. Jacobs, Journal of Magnetism and Magnetic Materials 92 (1990) L35.
[21] R. Coehoorn, G.H.O. Daalderop, Journal of Magnetism and Magnetic Materials 104–107 (1992) 1081.
[22] S.S. Jaswal, IEEE Transaction on Magnetics 28 (1992) 2322.
[23] Z. Gu, W. Lai, Journal of Applied Physics 71 (1992) 3911.
[24] H. Fujii, I. Sasaki, K. Koyama, Journal of Magnetism and Magnetic Materials 242–245 (2002) 59.
[25] H. Fujii, K. Koyama, K. Tatami, S. Mitsudo, M. Motokawa, T. Kajitani, Y. Morii, P.C. Canfield, Physica B 237–238 (1997) 534.